

Sc.D. Thesis Summary

FISCHER-TROPSCH SYNTHESIS IN A SLURRY REACTOR

by

George Albert Huff, Jr.

Abstract

The intrinsic kinetics and organic product selectivity of the Fischer-Tropsch synthesis were studied in a mechanically-agitated, one-liter autoclave with an alkalized, fused-iron (ammonia synthesis) catalyst. Reaction conditions varied from 232 to 269°C, total pressure of 275 to 1480 kPa, reactant feed rates of 1100 to 8500 volume synthesis gas (at S.T.P.)/hr/volume catalyst, and H₂/CO feed ratios of 0.34 to 1.81. No significant loss in activity or change in catalyst selectivity was noted for as much as 30 days on stream.

The rate of synthesis was found to be near first order in hydrogen concentration, zero order in carbon monoxide concentration, and strongly inhibited by water. Langmuir-Hinshelwood kinetic models fitted the data quite well with an activation energy of 20 kcal/mol. The water-gas-shift reaction proceeded to equilibrium at the higher temperatures.

The principal product at each carbon number was normal paraffins and alpha olefins. Smaller amounts of oxygenates (mostly normal alcohols) and branched hydrocarbons were obtained. Little secondary olefin hydrogenation or oxygenate dehydration occurred with C₃+ products; the inlet H₂/CO ratio and hydrogen partial pressure had the greatest affect on product selectivity.

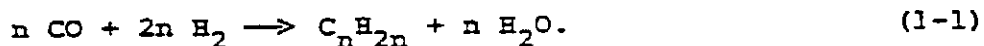
The Flory distribution curve to C₅₀ appeared to have three values of chain growth probability α . The product was dominated by paraffins at the highest carbon numbers ($\alpha = 0.93$) and by olefins at intermediate carbon numbers ($\alpha = 0.75$). With the C₁ to C₉ fraction, which constituted about 90 mole % of the organic product, all components exhibited about the same value of α which varied slightly with operating conditions (0.62 to 0.71). Higher molecular-weight products were selectively retained in the liquid carrier. Therefore, distributions based only on the vapor-phase composition can be misleading, especially during the early stages of a run.

I. Summary

I. A. Introduction

Large increases in crude oil prices since the early 1970's, coupled with the realization that indigenous petroleum reserves are dwindling, has renewed interest in the production of liquid transportation fuels from the immense reserves of coal that exist in the United States. One such indirect liquefaction method is the Fischer-Tropsch synthesis in which carbon monoxide and hydrogen, products of coal gasification, are catalytically converted to a mixture of primarily linear paraffins and olefins with some oxygenates (mostly alcohols). Over an iron catalyst, the synthesis is typically carried out between 200 to 300°C and total pressures of 450 kPa (50 psig) to 2.2 MPa (300 psig).

The reaction stoichiometry is approximately represented by:



Two important side reactions can occur concurrently with the synthesis. Water, formed as a primary product of the synthesis, can react with carbon monoxide by the water-gas-shift reaction to generate hydrogen:



Carbon monoxide can disproportionate by the Boudouard reaction to produce elemental carbon on the catalyst surface:



Slurry reactors for this highly exothermic synthesis offer several potential advantages over the more conventional fixed- and fluidized-bed reactors:

- 1) They provide a uniform temperature throughout the reactor as the liquid provides excellent heat transfer. This is particularly important since carbon deposition is aggravated by higher temperatures, such as "hot spots" that plague operation in fixed-bed reactors.
- 2) High mechanical strength of the catalyst is not required, whereas crush strength is essential in fixed-bed reactors and attrition resistance is vital in fluidized-bed reactors.
- 3) They can process synthesis gas of low hydrogen to carbon monoxide ratio, characteristic of thermally efficient coal gasifiers, without upgrading the hydrogen content as is necessary in other reactor types.

I. B. Objectives

The present study focused on the Fischer-Tropsch synthesis over an iron catalyst in a slurry-bed reactor. It was desired to determine the kinetics (free of heat and mass transfer limitations) of the Fischer-Tropsch synthesis under industrially relevant conditions, to obtain a fundamental understanding of the organic carbon number distribution, and to determine the factors which influence selectivity to oxygenates, olefins, and

paraffins. The basic approach was to investigate the effects of reaction variables, such as temperature, feed composition, total pressure, and reactant feed rate, on catalyst activity and product selectivity.

I. C. Literature Review

I. C. 1. Fischer-Tropsch Activity

The following conclusions can be drawn from semi-empirical treatment of rate data, obtained in fixed-bed, vapor-phase reactors over iron, in a number of different Fischer-Tropsch kinetic studies (Anderson, 1956; Anderson and Karn, 1960; Kōlbel et al., 1960; Dry, 1976; Atwood and Bennett, 1979; Thomson et al., 1980; Feimer et al., 1981):

- 1) The synthesis rate appears to increase with hydrogen partial pressure and to be independent of or increase slightly with carbon monoxide partial pressure.
- 2) Water inhibits the rate.
- 3) The overall activation energy is about 17 to 25 kcal/mol.

Most noteworthy is the rate expression proposed by Anderson (1956), based on unpublished work at the U.S. Bureau of Mines, as:

$$-R_{H_2+CO} = aP_{H_2} P_{CO} / (P_{CO} + bP_{H_2O}) \quad (1-4)$$

which reduces to a simple first-order dependency on hydrogen concentration at lower conversions:

$$-R_{\text{H}_2+\text{CO}} = aP_{\text{H}_2} \quad (1-5)$$

This latter equation was verified by Dry et al. (1972) in a carefully-controlled investigation carried out in a fixed-bed reactor operated at low conversion in a differential mode. Note that when the rate of hydrocarbon synthesis by the Fischer-Tropsch reaction (Eqn. 1-1) is based on the moles of hydrogen plus carbon monoxide converted ($-R_{\text{H}_2+\text{CO}}$), it is independent of the rate of the water-gas-shift reaction (Eqn. 1-2) since one mole of hydrogen is formed for each mole of carbon monoxide consumed. Of course, it is assumed that the rate of carbon monoxide decomposition by the Boudouard reaction (Eqn. 1-3) is negligible.

I. C. 2. Carbon Number Distribution

The synthesis of hydrocarbons by the Fischer-Tropsch reaction can be viewed as starting from an initial single-carbon unit which can either grow in molecular size by addition of another carbon unit or terminate and desorb into the gas (or liquid) phase as product. Although the type of carbon unit that initiates this process is the object of considerable controversy (Anderson, 1956; Ponec, 1978; Rofer-DePoorter, 1981), its exact nature does not affect the mathematical development of an expression to predict the carbon number

distribution provided that the probability of chain growth remains independent of molecular size. The basic relationship was statistically derived by Flory (1936) for any polymerization process in which the primary step is the addition of a monomer (a single carbon unit for Fischer-Tropsch) one at a time onto the terminus of a growing linear chain, and one polymer molecule is produced from each kinetic chain. The mole fraction m_n of molecules in the polymer mixture which contain n structural units is given by:

$$m_n = (1 - \alpha) \alpha^{n-1}, \quad (1-6)$$

which on a weight fraction w_n basis becomes:

$$w_n = (1 - \alpha)^2 n \alpha^{n-1}. \quad (1-7)$$

The chain growth probability factor α is defined as:

$$\alpha = r_p / (r_p + r_t), \quad (1-8)$$

where r_p and r_t are the rates of propagation and termination, respectively. The logarithmic form of the Flory distribution (Eqn. 1-6) is a more convenient form with which to express experimental data:

$$\ln (m_n) = n \ln (\alpha) + \ln \left(\frac{1 - \alpha}{\alpha} \right). \quad (1-9)$$

Thus, a plot of $\ln (m_n)$ should be linear with carbon number n . The probability of chain growth α may be obtained from either the slope (as $\ln (\alpha)$) or the ordinate intercept (as $\ln(1 - \alpha)$ at $n = 1$).

Application of the Flory distribution to the limited Fischer-Tropsch data available over iron has met with only

partial success. Although C_3+ data for hydrocarbons generally fit Eqn. (1-9), the C_2 fraction is usually reported to be "lower than expected" and the CH_4 fraction to be "higher than expected". Until recently, these observations were explained by postulating that ethylene has a greater activity for re-incorporation into growing chains on the catalyst surface (Schulz et al., 1970), and methane was considered to be formed by additional mechanisms such as cracking (Henrici-Olivé and Olivé, 1976). However, Satterfield and Huff (1982-a) pointed out that this behavior probably stemmed instead from consideration of only certain groups of products, such as hydrocarbons, rather than the entire product spectrum. When oxygenates were included, C_1 and C_2 products fell on the same line as higher carbon numbers. However, other deviations from the Flory distribution cannot be easily dismissed. Such is the case for results reported by Weingaertner (1956) in which the data appear to fit two straight lines, the first from C_1 to C_{11} ($\alpha = 0.70$) and the second for $C_{12}+$ ($\alpha = 0.37$). No explanation for this behavior has appeared in the literature.

I. D. Experimental

Synthesis gas was passed continuously through a mechanically-stirred autoclave about half-filled with a low volatile, inert liquid, normal-octacosane, in which the finely divided catalyst was suspended. The versatile system can be employed for fundamental intrinsic kinetic studies, such as those reported

here, in which the entire contents are well mixed so that no gradients of concentration or temperature exist through the reactor, or it can be operated under conditions controlled by the degree of gas-to-liquid mass transport (Satterfield and Huff, 1982-b).

I. D. 1. Reactor

The slurry reactor and ancillary equipment are schematically depicted in Fig. 1-1. The stainless-steel, 1-liter autoclave was operated in a semibatch fashion; synthesis gas was continually sparged to the slurry in the reactor while volatile products were removed overhead, whereas the catalyst and inert liquid remained in the reactor for the duration of a run (up to 30 continuous days on stream). No heat or mass transfer limitations were present, as evidenced by a negligible change in conversion at faster stirring speeds or by changing the feed location in the reactor. These effects also indicated that the reactor contents were well mixed. After an initial period, steady-state operation with regard to catalytic activity and selectivity was obtained over the entire run. Experimental parameters studied are summarized in Table 1-1. Space velocities reported are calculated as inlet gas volumetric flow rate at S.T.P. divided by the volume of catalyst on an unreduced basis, assuming a bed density of 2.6 g/cm^3 .

I. D. 2. Catalyst and Liquid Carrier

The catalyst (from United Catalysts, Inc. and designated C-73) was a fused magnetite normally employed for ammonia synthesis. On an unreduced basis, it contained 2.0-3.0% Al_2O_3 , 0.5-0.8% K_2O , 0.7-1.2% CaO , and $< 0.4\%$ SiO_2 . A quantity of about 75 g was crushed to particle sizes smaller than 90 microns and prereduced in a separate vessel with hydrogen at 400°C , atmospheric pressure, and space velocity of $10,000 \text{ hr}^{-1}$. It was then slurried with about 400 g of the liquid carrier ($n\text{-C}_{28}\text{H}_{58}$ of $> 99.9\%$ purity) to produce about a 16-wt % suspension, based on unreduced weight. By the use of pure octacosane in the reactor, the accumulation of high molecular-weight products could be clearly distinguished from the starting material.

I. D. 3. Product Analysis

Liquid hydrocarbons and water were condensed in two traps, one operated at about 65°C , and the second at 2°C . In each trap the liquid separated into an oil phase which contained the bulk of the hydrocarbon product and an aqueous phase consisting of water plus oxygenates. These fractions together with the residual gas were analyzed by gas chromatography. Details of this procedure are published elsewhere (Buff et al., 1982). Because of the tremendous number of compounds produced, they are lumped here for discussion into four categories -- oxygenates

(mostly normal alcohols), alpha plus beta olefins, normal paraffins, and "remainder" which is composed primarily of branched isomers with a few cyclics. The degree of unsaturation in this later category is not known as individual components were not readily identifiable by mass spectroscopy. For the total of the C_1 to C_{10} fraction, the product composition amounted typically to about 45 mole % of α - (predominately) and β -olefins, 35 mole % normal paraffins, 15 mole % oxygenated hydrocarbons, and 5 mole % remainder.

Molecular oxygen material balances typically closed between 98 to 102% but only 90 to 95% of molecular hydrogen and carbon fed to the reactor could be accounted for in overhead products. The remainder stayed in the liquid carrier. At the highest H_2/CO feed ratio of 1.81 where little elemental carbon should be formed by the Boudouard reaction, the molar ratio of unaccounted for carbon to molecular hydrogen averaged 1.04. In other words, hydrocarbon product accumulated in the reactor, assuming that the product was C_nH_{2n} per Eqn. (1-1).

I. E. Results

I. E. 1. Synthesis Gas Disappearance

Fig. 1-2 shows the dependency of the rate of hydrogen plus carbon monoxide disappearance at 232°C on hydrogen partial pressure. With conditions ranging from total pressures of 445 to 1480 kPa, H_2/CO feed ratios of 0.55 to 1.81, space velocities

of 1500 to 4000 hr^{-1} , hydrogen conversion varied from 17 to 65% and carbon monoxide conversion from 16 to 87% for the results depicted in the figure. Most of the data are well fitted by a simple first-order dependency of rate on hydrogen concentration and independent of carbon monoxide concentration. Those results which significantly deviate from the relationship were taken under conditions where the effluent water partial pressure was higher than 0.1 atm (10 kPa). These observations are qualitatively consistent with the semi-empirical rate expression given by Eqn. (1-4) for vapor-phase reactors. In terms of a Langmuir-Hinshelwood formulation, this would imply that water and carbon monoxide effectively saturate the surface and compete with one another for active sites on the catalyst. Data at higher temperatures show similar behavior except that fewer points lie on the straight line due to increased conversion.

The data also indicate that the water-gas-shift reaction is near equilibrium, which is well to the right as written in Eqn. (1-2). At 269°C, the term $P_{\text{H}_2} P_{\text{CO}_2} / P_{\text{CO}} P_{\text{H}_2\text{O}}$ varies from 53 to 58 compared to a theoretical equilibrium value of 62. Differences are attributed to experimental error in water measurement. At 232°C, the water-gas-shift is kinetically limited as the term $P_{\text{H}_2} P_{\text{CO}_2} / P_{\text{CO}} P_{\text{H}_2\text{O}}$ varies from 12 to 74 in contrast to a value of 119 if equilibrium had been achieved.

I. E. 2. Organic Product Carbon Number Distribution

A detailed carbon number distribution, typical of those obtained over the fused-iron catalyst, is plotted in Fig. 1-3

for Run 9-45 after 620 hours on stream at 263°C and total pressure of 790 kPa, in which hydrogen and carbon monoxide conversions were 60 and 62%, respectively. The data are plotted as the logarithm of the ratio of moles at carbon number n to the accumulative moles of organic from C_1 to C_{27} , termed mole fraction m_n , versus carbon number. This distribution is for volatile products collected overhead from the reactor and therefore does not account for accumulation of low volatile components in the liquid carrier.

As seen in the figure, the slope of the curves for $\alpha + \beta$ -olefins and for hydrocarbon remainder (mostly branched compounds) are nearly identical and so these components can be combined when modeling the total carbon number distribution. The ratio of $\alpha + \beta$ -olefins plus remainder to n -paraffins is plotted at the bottom of the figure and given by the right-hand ordinate.

The continual drop-off of the $C_{20}+$ product in the plot is due to significant accumulation of lower volatility material in the liquid carrier, as shown by analysis of the liquid carrier at the end of Run 9, 60 hours later (Fig. 1-4). Although the liquid carrier was initially pure n -octacosane, it now contained more than 14-wt % of $C_{50}+$ hydrocarbons and less than 56-wt % of C_{28} . A maximum is reached for the conditions of Run 9 at C_{24} , above which most of the product remains in the reactor. This peak corresponds to about the same carbon number at which products collected overhead (Fig. 1-3) begin to tail off. For the present, only the results below C_{19} will be considered as they are unaffected by this artifact.

At carbon numbers greater than C_2 in Fig. 1-3, the slope of each organic class is constant over a wide range of carbon numbers. This agrees with findings that secondary reactions between organic groups for $n > 2$ are minimal. For example, Summerhayes (1982) has individually added butene-1 and ethylene to the feed in this same system but found no evidence for olefin re-incorporation into the growing chains, although some secondary hydrogenation of ethylene to ethane occurred.

At a carbon number of about 10 in the figure, there is a marked change in product selectivity. Below C_{10} , the slope of each organic group is about the same. The total organic curve from C_1 to C_9 can be fitted by a straight line from which the slope and intercept give the same value of $\alpha = 0.68$ (Eqn. 1-9). Since the cumulative C_1 to C_9 fraction comprises about 95 mole % of the organic collected for Run 9-45, the error in neglecting the $C_{10}+$ material is small. The values of α from the slope and intercept agree. This internal check implies that the Flory distribution is followed to C_{10} . Above C_{10} , the slope for normal paraffins becomes much lower than that for the other hydrocarbons. This transition is readily seen in the ratio of (olefin + remainder)/paraffin at the bottom of the figure. This change in organic selectivity affects only hydrocarbons as the oxygenate slope remains constant.

The change at C_{10} is believed to be caused by the catalyst having more than one probability of chain growth α . If there were two sites for organic synthesis on the catalyst that were assumed to be non-interacting, the Flory expression (Eqn. 1-6) becomes:

$$m_n = \underbrace{x(1-\alpha_1)\alpha_1^{n-1}}_{\text{Site 1}} + \underbrace{(1-x)(1-\alpha_2)\alpha_2^{n-1}}_{\text{Site 2}} \quad (1-10)$$

where:

m_n = the total moles of carbon number n relative to the total moles of organic product

α_1, α_2 = the probabilities of chain growth for the two sites

x = the mole fraction of organic synthesized on the first site

A generalized plot of Eqn. (1-10) is illustrated in Fig. 1-5 where $\alpha_2 > \alpha_1$. Since the mole fraction is on a logarithmic basis in a Flory plot, the transition from most of the products synthesized on Site 1 to Site 2 at C_{10} is abrupt. An "S" shaped curve results as heavier products ($C_{20}+$) begin to accumulate significantly in the liquid carrier with a corresponding decrease in the mole fraction observed overhead.

The establishment of steady-state with respect to the heavier organic product is a slow process, as observed experimentally (Fig. 1-6), because both vapor pressure and the product mole fraction decrease logarithmically with carbon number. The "S" shaped curve becomes more pronounced with time on-stream as an increasing fraction of heavy components synthesized on the second site saturate the liquid carrier and appear overhead.

The effect of accumulation may be more easily understood by looking at Fig. 1-7 in which characteristic times have been

calculated for a specified fraction of carbon number n to have volatilized from the reactor. This was based on the same reaction conditions of Run 9-45 depicted in Fig. 1-3, assuming that equilibrium is established between the liquid carrier and effluent vapor at 263°C and 790 kPa. For example, at 0.65 hours after start of run, 30% of the total C_{10} synthesized is predicted to have been volatilized out of the reactor; at 8 hours, 90% of the total should have appeared overhead. At times of interest here (100 to 700 hours on stream), the $C_{20}+$ fraction is expected to be significantly affected by accumulation of less volatile components, as confirmed by the experimental results shown in Fig. 1-3 and 1-4. Hence, the product distributions obtained overhead from a Fischer-Tropsch slurry reactor at early run times can be misleading.

I. F. Discussion of Results

I. F. 1 Intrinsic Rate Expressions for the Fischer-Tropsch Synthesis

From empirically-derived kinetic expressions reported in the literature (such as Eqn. 1-4), guidelines can be developed to assist in deriving more fundamental, Langmuir-Hinshelwood rate expressions:

- 1) The rate-determining step appears to be the reaction of hydrogen with a carbon intermediate to form a complex which then rapidly polymerizes.

- 2) Carbon monoxide and water effectively compete for available catalytic sites so as to saturate the surface. The rate is inhibited by water formation while under differential conditions it becomes zero order with respect to carbon monoxide.
- 3) Since the differential rate is first order in hydrogen partial pressure and not one-half, hydrogen dissociates (if at all) onto only one catalytic site.
- 4) If the rate-determining step were the bimolecular reaction between an adsorbed hydrogen and carbon complex that involved two catalytic sites, the rate should show a negative order dependence (under differential conditions) with carbon monoxide concentration (which saturates) and not zero order, as observed (Eqn. 1-5). Hence, the rate-determining step appears to involve only a single site.

From a mathematical standpoint, this last observation is consistent with a mechanism that involves an unadsorbed hydrogen molecule reacting directly with adsorbed complexes (Dry et al., 1972). Alternately, two types of adsorption sites could exist; one that constitutes the majority of the metal surface on which carbon monoxide strongly adsorbs and hydrocarbon chains grow, and the other on which only hydrogen weakly adsorbs. The fractional surface coverage of hydrogen would then be proportional to partial pressure (Vannice, 1975).

Two mathematically different Langmuir-Hinshelwood kinetic models, allowing for adsorptivities of carbon monoxide and

water, can be derived. The first involves the reaction of hydrogen with adsorbed carbon monoxide to form an adsorbed COH_2 complex, and carbon monoxide and water are assumed to be the most abundant surface intermediates (Dry, 1976):

$$-R_{\text{H}_2+\text{CO}} = kK_{\text{CO}}P_{\text{CO}}P_{\text{H}_2} / (1 + K_{\text{CO}}P_{\text{CO}} + K_{\text{H}_2\text{O}}P_{\text{H}_2\text{O}}) \quad (1-11)$$

where k and K denote the intrinsic rate constant and adsorption equilibrium constant, respectively. Another expression can be derived by taking the rate-determining step to be the reaction of an adsorbed COH_2 specie (formed rapidly from CO and H_2) with hydrogen to form an adsorbed CH_2 intermediate, and COH_2 and H_2O are assumed to saturate the surface:

$$-R_{\text{H}_2+\text{CO}} = kK_{\text{CO}}K_{\text{COH}_2}P_{\text{CO}}P_{\text{H}_2}^2 / (K_{\text{H}_2\text{O}}P_{\text{H}_2\text{O}} + K_{\text{CO}}K_{\text{COH}_2}P_{\text{CO}}P_{\text{H}_2}). \quad (1-12)$$

Alternately, this same type of mathematical relationship can be formulated by assuming that carbon monoxide dissociates on the surface to carbon and oxygen and that carbon reacts with hydrogen in the rate-determining step where adsorbed carbon is the most abundant surface component.

Both models well fit experimental data taken over temperatures of 232 to 263°C, pressures at 275 to 1480 kPa, space velocities of 1500 to 4000 volume synthesis gas (at S.T.P.) / hr/volume unreduced catalyst, and H_2/CO feed ratios of 0.34 to 1.81. This range of conditions produced a hydrogen conversion of 17 to 74% and carbon monoxide conversion of 16 to 98%. The calculated activation energy and heat of

adsorption for the terms of each model are summarized in Table 1-2. A "t" test analysis between the predicted rate and that experimentally observed showed that the two models were statistically indistinguishable at a 95% confidence limit, even though Eqn. (1-12) has only two adjustable parameters while Eqn. (1-11) requires three.

The activation energies of 20 and 21 kcal/mol (Table 1-2) agree with values reported for iron catalysts in fixed-bed, vapor-phase reactors of 17 to 25 kcal/mol. The heat of adsorption for carbon monoxide in Eqn. (1-11) of +31 kcal/mol is within the range reported for chemisorption studies of +32 kcal/mol at low coverages (less than 10% of the surface) to +10 kcal/mol at higher coverages (about 60% of the surface) (Dry et al., 1969). While no values have been reported for water, a high heat of adsorption (Satterfield, 1980) implies that it may be reacting with the catalyst surface and is no longer confined to a chemisorbed surface layer. Although the heat of adsorption for the group $K_{CO}K_{COH_2}/K_{H_2O}$ of Eqn. (1-12) is negative, recall that this is a lumped term which simply implies that the heat of adsorption of water is +24 kcal/mol larger than the combined value for CO and COH₂.

I. F. 2. Dual Organic Synthesis Site

For carbon numbers below 9 or 10 in Fig. 1-3, the probability of chain growth, based on slope, for all components is about the same ($\alpha = 0.68$). Since the C₁ to C₉ fraction

comprises more than 90 mole % of the total organic product, it is not surprising then that Satterfield and Huff (1982-a) have observed that α for the overall product (oxygenates plus hydrocarbons) is insensitive to reaction conditions even though the relative fractions of paraffins, olefins, branched compounds, and oxygenates change. However, a marked change in selectivity occurs at C_9 or C_{10} as the probability for chain growth increases for the C_{11} to C_{20} hydrocarbon fraction, reflected by the slope of the curves in Fig. 1-3, while that for oxygenates remains unchanged. The α for paraffins is now 0.94 which is much greater than that of 0.77 observed for olefins and hydrocarbon remainder over this same carbon number range. The product mole fraction observed overhead drops-off above C_{20} because of accumulation in the liquid carrier.

If accumulation of components in the reactor is ignored, the curves between C_{11} to C_{20} could be extrapolated to C_{20}^+ (Fig. 1-8), assuming that there were no further irregularities in the distribution. In Fig. 1-8 olefins have been combined with remainder since they have the same α for C_{10}^+ (Fig. 1-3). Recall that the total organic is the summation of oxygenates, paraffins, olefins, and remainder and that the α of the total at carbon number n reflects the dominant component. The total organic curve in Fig. 1-8 shows three distinct slopes or probabilities of chain growth, as indicated by Regions I, II and III. Below C_9 (Region I), the α value for all components, and hence the total, is 0.68. In Region II, olefins plus remainder are the major group and so the total organic follows

this curve with $\alpha = 0.77$. Paraffins eventually become the major product (about C_{20}) since their chain growth probability of 0.94 is considerably greater than that of 0.77 for olefins plus remainder. As a result, the total organic at $C_{20}+$ (Region III) is postulated to fit an α value of 0.94. This region is not observed in product distributions for organic collected overhead from the reactor (Fig. 1-3) due to significant accumulation of heavy components in the liquid. However, analysis of the liquid carrier (Fig. 1-4) revealed that $\alpha = 0.93$ for C_{24} to C_{50} total compounds, which is in excellent agreement with that expected in Fig. 1-8 of 0.94.

The noticeable change in the probabilities of chain growth at C_{10} suggests that product is synthesized over more than one type of site; some growing chains are strongly adsorbed on the catalyst to produce high molecular weight products while others are weakly bound and form mostly lighter products. This is based on the following key observations in the organic product distribution of Fig. 3-1, neglecting accumulation effects:

- 1) The slope for oxygenates is constant from C_3+ .
- 2) From C_1 to C_9 , the slope for (i) olefins plus remainder, (ii) oxygenates, and (iii) paraffins is about the same ($\alpha = 0.68$).
- 3) At $C_{10}+$, both the slope for paraffins and olefins plus remainder decreases. However, the slope for paraffins ($\alpha = 0.94$) is lower than that for olefins plus remainder ($\alpha = 0.77$), as seen in Fig. 1-8.